over Hawaii and near Mexico City are a known artifact of the CAMSRA related to volcanic outgassing. Figure 2.50c shows a simple indicator of the occurrence of extreme monthly AOD values. The region most impacted was around Iran and Pakistan and, to a lesser extent, the rest of the Middle East and the Arabian Sea, due to a series of dust storms from April to June. The high values over southern Canada, the western United States, and parts of the North Atlantic are associated with extreme fires in August and November.

Radiative forcing resulting from aerosol–radiation (RFari) and aerosol–cloud interactions (RFaci) for the period 2003–18 is shown in Fig. 2.51, as estimated using the methods described in Bellouin et al. (2013) but with CAMSRA data. The year 2018 was average in terms of RFari, while RFaci was relatively weak due to fewer anthropogenic aerosols over the ocean, where clouds are more sensitive to aerosol perturbations. Trends remain statistically fragile because of large uncertainties in the estimates.

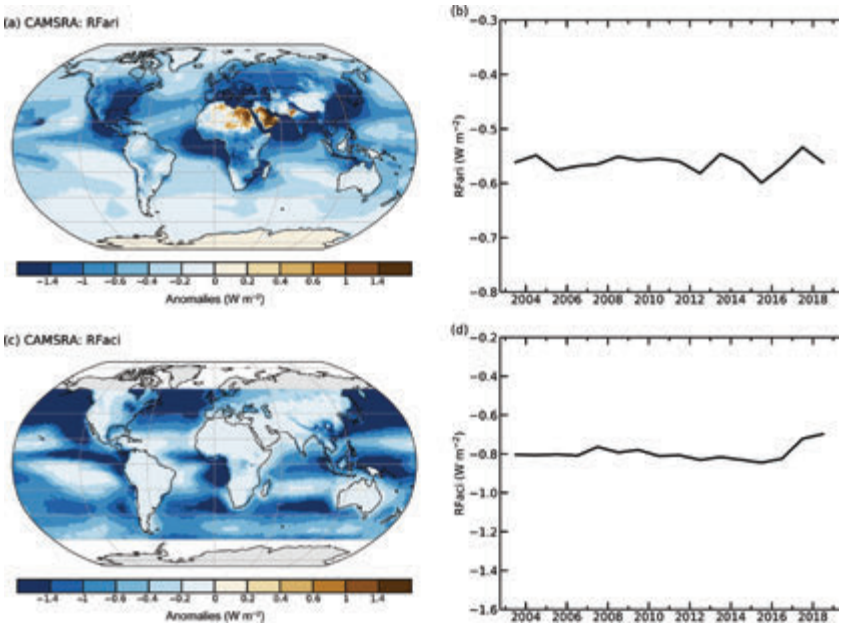

Fig. 2.51. Radiative forcing in the shortwave spectrum of (a), (b) aerosol-radiation (RFari) and (c), (d) aerosol-cloud interactions (RFaci) from 2003–18. Negative radiative forcings imply a cooling effect of the aerosols on the climate; absorbing anthropogenic aerosols exert positive RFari over bright surfaces, like the African and Arabian deserts, as shown in the upper panel.

4) Stratospheric ozone—M. Weber, W. Steinbrecht, C. Arosio, R. van der A, S. M. Frith, J. Anderson, M. Coldewey-Egbers, S. Davis, D. Degenstein, V. E. Fioletov, L. Froidevaux, D. Hubert, C. S. Long, D. Loyola, A. Rozanov, C. Roth, V. Sofieva, K. Tourpali, R. Wang, and J. D. Wild

Global stratospheric ozone levels vary from year to year depending on the dynamical state of the atmosphere. Generally, ozone variability becomes larger with increasing latitude. Plate 2.1aa shows the global distribution of annual mean total ozone anomalies for 2018. Total ozone variability in the tropics is mainly governed by the Quasi-bienniel Oscillation (QBO). During NH winter 2017/18, the QBO at 50 hPa (~22 km, lower stratosphere) was in its easterly phase. This is associated with negative total ozone anomalies in the inner tropics (e.g., Diallo et al. 2018) and positive anomalies in the subtropics and midlatitudes. Throughout the entire SH extratropics, total ozone levels in 2018 were, therefore, well above the mean [up to 15 Dobson units (DU)] compared to the reference period 1998–2008. Over much of the Antarctic region, values were lower than the long-term mean. This is related to an above-average size spring ozone hole in 2018 (see low October means in Fig. 2.52e and Section 6j). Extratropical ozone variability maximizes in winter/spring when meridional ozone transport related to the Brewer-Dobson circulation and QBO is most active. These transport variations are the main contributors to variations in annual mean total ozone. In the NH, therefore, total ozone was slightly above average in 2018 but with extended regions of negative anomalies. Above the Aleutian region in Alaska, total ozone was up to 15 DU below the long-term average, while above Greenland and the North Atlantic region, total ozone was higher by more than 15 DU (Plate 2.1aa). In spring 2018, NH polar ozone losses were largely absent due to warm conditions (and enhanced ozone transport) and a weak polar vortex (North Atlantic region). The March NH polar cap total ozone mean in 2018 (Fig. 2.52e) was in the upper range of values observed during the last two decades.

Figure 2.52 shows the annual mean total ozone time series from various merged datasets for the near-global average (60°N–60°S) average, tropics, extratropics, and selected months in the polar regions. Midlatitude total ozone means were high in 2018, while the tropical values were low compared to the annual means observed in the recent decade (see also

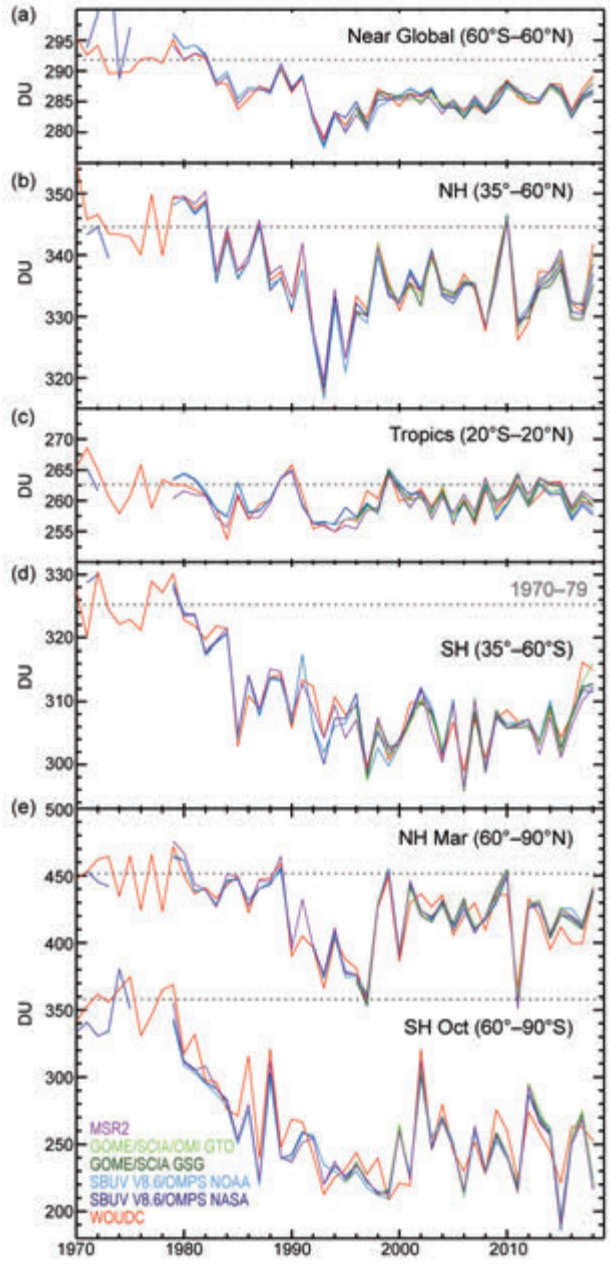

Fig. 2.52. Time series of annual mean total ozone (DU) in (a)–(d) four zonal bands, and (e) polar (60°–90°) total ozone in Mar (NH; see also Section 5j) and Oct (SH), the months when polar ozone losses usually are largest. Data are from WOUDC (World Ozone and Ultraviolet Radiation Data Centre) ground-based measurements combining Brewer, Dobson, SAOZ (Système D'Analyse par Observations Zénithales), and filter spectrometer data (red: Fioletov et al. 2002, 2008); the BUV/SBUV/SBUV2 V8.6/OMPS merged products from NASA (MOD V8.6, dark blue, Frith et al. 2014, 2017) and NOAA (light blue: Wild and Long, personal communication, 2019; the GOME/SCIAMACHY/GOME-2 products GSG from University of Bremen (dark green, Weber et al. 2018) and GTO from ESA/DLR (light green, Coldewey-Egbers et al. 2015; Garane et al. 2018). MSR-2 (purple) assimilates nearly all ozone datasets after corrections with respect to the ground data (van der A et al. 2015). All six datasets have been bias corrected by subtracting averages for the reference period 1998–2008 and adding back the mean of these averages. The dotted gray lines in each panel show the average ozone level for 1970–79 calculated from the WOUDC data. All data for 2018 are preliminary.

Plate 2.1aa). For all latitude bands, except the tropics, the average total ozone levels have not yet recovered to the values of the 1970s, a time when ozone losses due to ozone-depleting substances (ODSs) were still very small (WMO 2018a). A recent study by Weber et al. (2018) indicates that total ozone trends since the late 1990s are positive (<1% decade^{-1}), but at most latitudes the trends do not reach statistical significance. Still, the small increase in global total ozone following the significant decline before the 1990s provides proof that the Montreal Protocol and its Amendments, responsible for phasing out ODSs, has been successful. The observed changes in total ozone and in lower stratospheric ozone are reproduced well by state-of-the-art chemistry-transport model calculations that account for changes in transport and for changes in the ODSs regulated by the Montreal Protocol (Chipperfield et al. 2018).

Apart from the polar regions, the largest effect of ODSs occurs in the upper stratosphere (around 40 km altitude). Figure 2.53 shows an update of observed and modeled evolution of ozone at these altitudes and northern midlatitudes (e.g., Steinbrecht et al. 2017; WMO 2018a; SPARC/IO3C/GAW 2019). The ozone decline from the late 1970s to the late 1990s, due to increasing atmospheric concentrations of ODSs, stopped. Since around 2000, ozone has been increasing slowly in both hemispheres, indicating success of the Montreal Protocol, and more or less as expected from model simulations, e.g., within the Chemistry Climate Model Initiative (CCMI; Dhomse et al. 2018; WMO 2018a; SPARC/IO3C/GAW 2019). At northern midlatitudes, ozone in 2018 was within the range observed in recent years.

Figure 2.54 shows that ozone profile trends vary with longitude. The largest (and most significant) ozone increases from 2003–18 have occurred between 40 km and 45 km altitude in the Western Hemisphere, and at higher latitudes in both hemispheres. Longitudinal variations arise from zonally non-symmetric changes in circulation patterns, which influence trace gas transports and chemical reactions relevant for ozone. More studies are needed to consolidate these results and their interpretation.

In the lower stratosphere, ozone variations are largely driven by meteorological

variations in transport, and less so by changes in ODSs (e.g., Chipperfield et al. 2018). Ozone near 50-hPa/22-km altitude at midlatitudes in both hemispheres declined before the mid-1990s and remained more or less stable during the last 20 years (Fig. 2.53c). In the tropics (e.g., 20°N–20°S), observations and CCMI model simulations at 50 hPa do show a continuing long-term decline, which is linked to a climate

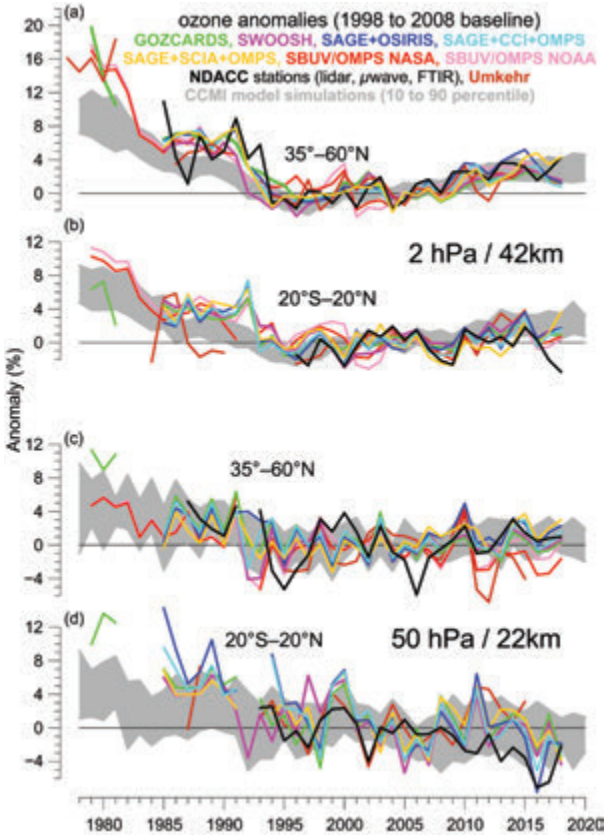

Fig. 2.53. Annual mean anomalies of ozone in the upper stratosphere near (a) and (b) 42 km altitude (2 hPa) and (c) and (d) near 22 km (50 hPa) for two zonal bands: 35°–60°N and 20°N–20°S (tropics), respectively. Anomalies are referenced to the 1998–2008 baseline. Colored lines are for long-term records obtained by merging different limb (GOZCARDS, SWOOSH, SAGE+OSIRIS, SAGE+CCI+OMPS-LP, SAGE+SCIAMACHY+OMPS-LP) or nadir viewing (SBUV, OMPS-NP) satellite instruments. Black line is from merging ground-based ozone records at NDACC stations employing differential absorption lidars, microwave radiometers, or Fourier Transform InfraRed spectrometers (FTIRs). Brown line is for ground-based Umkehr measurements. See Steinbrecht et al. (2017), WMO 2018a, and Arosio et al. (2018) for details on the various datasets. Gray shaded area shows the range of chemistry-climate model from CCMI (WMO 2018a; SPARC/IO3C/GAW 2019; Dhomse et al. 2018). Ozone data for 2018 are not yet complete for all instruments and are still preliminary.

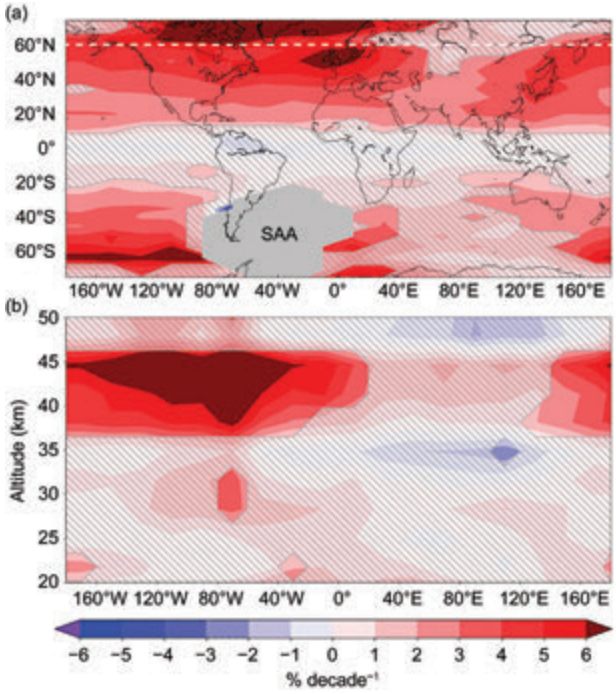

Fig. 2.54. Ozone trends (% decade^{-1}) at (a) 43.1 km for (latitude vs. longitude) and (b) 60°N (altitude vs. longitude) from the longitudinally resolved SCIAMACHY-OMPS-LP merged ozone profile dataset for the 2003–18 period as derived from a multiple variate linear regression. Dashed areas indicate non-significant trends and the gray polygon indicates the location of the South Atlantic Anomaly (SAA) where data quality is poor. Update from Arosio et al. 2018.

change-related acceleration of the meridional Brewer-Dobson circulation (Ball et al. 2018; Chipperfield et al. 2018; WMO 2018a). The large interannual variations and the uncertainties in the observational data records result in considerable spread for the time series to date, thus making reliable detection of small underlying trends rather difficult.

5) Stratospheric water vapor—S. M. Davis, K. H. Rosenlof, D. F. Hurst, H. B. Selkirk, and H. Vömel

Following several years of dramatic changes in lower stratospheric water vapor (SWV), 2018 started as a relatively quiescent year. In January, the tropical mean (15°N–15°S) water vapor anomaly in the lowermost stratosphere (at 82 hPa), as measured by the *Aura* Microwave Limb Sounder (MLS) satellite instrument, was +0.14 ppm (parts per million mole fraction, equivalent to μmol mol^{-1}), which corresponds to a deviation of only 5% from its long-term 2004–18 average value for this month (2.9 ppm). From January through October this *Aura* MLS tropical mean lower stratospheric water vapor anomaly remained within 11% of its long-term average